analytical chemistry

Article

pubs.acs.org/ac

Isomerization Kinetics of AT Hook Decapeptide Solution Structures

Emily R. Schenk,[†] Mark E. Ridgeway,[‡] Melvin A. Park,[‡] Fenfei Leng,[†] and Francisco Fernandez-Lima*[,†]

[†]Department of Chemistry and Biochemistry, Florida International University, 11200 SW Eighth Street, AHC4-233, Miami, Florida 33199, United States

[‡]Bruker Daltonics, Inc., Billerica, Massachusetts 01821, United States

Supporting Information

ABSTRACT: The mammalian high mobility group protein HMGA2 contains three DNA binding motifs associated with many physiological functions including oncogenesis, obesity, stem cell youth, human height, and human intelligence. In the present paper, trapped ion mobility spectrometry-mass spectrometry (TIMS-MS) has been utilized to study the conformational dynamics of the third DNA binding motif using the "AT hook" decapeptide unit (Lys^1-Arg^2-$Prol^3$-Arg^4-Gly^5-Arg^6-$Prol^7$-Arg^8-Lys^9-Trp^{10}, ATHP) as a function of the solvent state. Solvent state distributions were preserved during electrospray ion formation, and multiple IMS bands were identified for the $[M + 2H]^{2+}$ and for the $[M + 3H]^{3+}$ charge states. Conformational isomer interconversion rates were measured as a function of the trapping time for the $[M + 2H]^{2+}$ and $[M + 3H]^{3+}$ charge states. Candidate structures were proposed for all IMS bands observed. Protonation site, proline residue conformation, and side chain orientations were identified as the main motifs governing the conformational interconversion processes. Conformational dynamics from the solvent state distribution to the gas-phase "de-solvated" state distribution demonstrated that ATHP is "structured", and relative abundances are associated with the relative stability between the proposed conformers. The most stable ATHP $[M + 2H]^{2+}$ conformation at the "de-solvated" state corresponds to the AT hook motif observed in AT-rich DNA regions.

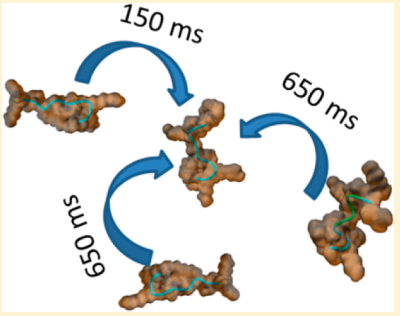

The mammalian high mobility group protein (HMGA2) is a multifunction nuclear transcription factor directly linked to oncogenesis,[1,2] obesity,[3,4] as well as human height,[5,6] stem cell youth,[7] and human intelligence.[8] HMGA2 is a small DNA-binding protein carrying three "AT hook" DNA binding motifs that specifically recognize the minor groove of AT-rich DNA sequences.[9] These DNA-binding motifs contain a consensus PRGRP sequence, flanked on each side by one of the positively charged amino acids, i.e., arginine or lysine. In the absence of AT-rich DNA, the "AT hook" DNA-binding motif is commonly assigned as "unstructured".[10,11] However, upon binding to the minor groove of five AT base pairs, it adopts a defined conformation.[11,12] This disorder-to-order structure transition in HMGA2 accounts for a variety of nuclear activities, such as transcription, recombination, and DNA replication.[8,9,12−14]

With the advent of soft ionization techniques (e.g., electrospray ionization, ESI[14]), traditional structural analysis of biomolecules (e.g., circular dichroism, CD, and nuclear magnetic resonance spectroscopy, NMR) can be highly complemented with measurements of ion-neutral collision cross sections (CCSs) using ion mobility spectrometry (IMS).[15−20] In particular, it has been shown that evaporative cooling of the solvent leads to a freezing of multiple conformations,[20,21] which can be further experimentally analyzed and compared with theoretical calculations of candidate structures.[21−23] With the recent introduction of trapped ion mobility spectrometry (TIMS),[24,25] the latter studies can be extended as a function of the trapping time inside the IMS cell, thus permitting isomerization kinetic measurements. In the current study, it is reported for the first time the isomerization kinetics of a truncated form of HMGA2 containing the third DNA binding motif: a decapeptide consisting of Lys^1-Arg^2-$Prol^3$-Arg^4-Gly^5-Arg^6-$Prol^7$-Arg^8-Lys^9-Trp^{10} (ATHP). The kinetic studies demonstrate that AT hook peptides can adopt multiple conformations in solution that vary according to charge state.

EXPERIMENTAL SECTION

The "AT hook" decapeptide unit (Lys^1-Arg^2-$Prol^3$-Arg^4-Gly^5-Arg^6-$Prol^7$-Arg^8-Lys^9-Trp^{10}, ATHP) was purchased from Advanced ChemTech Inc. (Louisville, KY) and used as received. Details on the TIMS-MS can be found elsewhere.[24,25] Briefly, a TIMS analyzer was coupled to a maXis Impact Q-UHR-TOF (Bruker Daltonics Inc., Billerica, MA). Data acquisition was controlled using in-house software, written in National Instruments Lab VIEW, and synchronized with the maXis Impact acquisition program. Nitrogen was used as the bath gas at ∼300 K. All samples were prepared at 1 μM concentration using HPLC grade solvents from Thermo Fisher Scientific Inc. (Waltham, MA). Mobility calibration and the number of isomer bands were determined using tune mix calibration standard (G2421A, Agilent Technologies, Santa Clara, CA) that comprises sphere-like structures that can only

Received: October 17, 2013
Accepted: December 23, 2013
Published: December 23, 2013

   dx.doi.org/10.1021/ac403386q | *Anal. Chem.* 2014, 86, 1210−1214

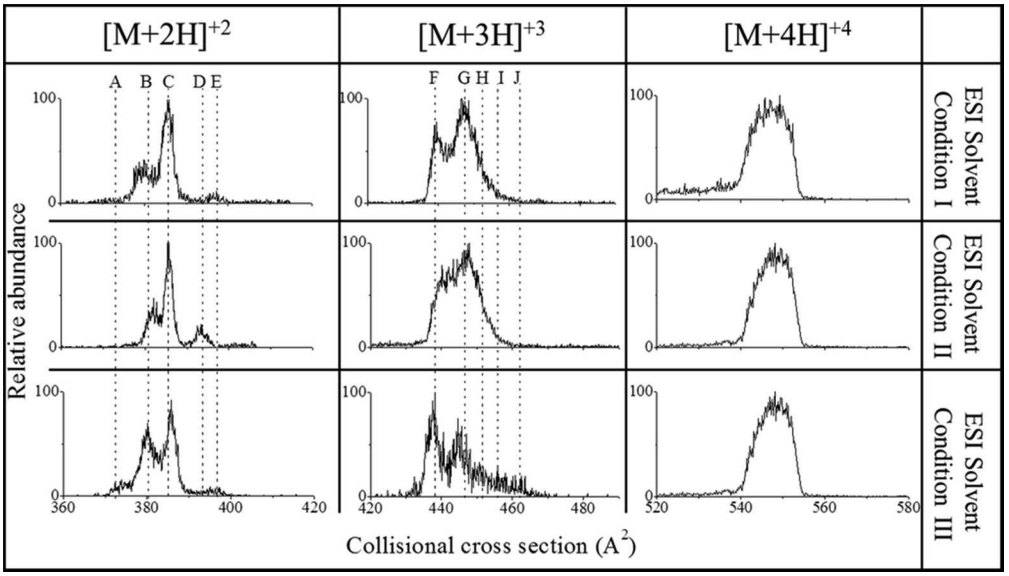

Figure 1. Typical ATHP $[M + 2H]^{2+}$, $[M + 3H]^{3+}$, and $[M + 4H]^{4+}$ CCS profiles as a function of the ESI solvent conditions (I) water/methanol/acetonitrile (33:33:33), (II) water/methanol/acetic acid (49:49:2), and (III) 10 mM ammonium acetate. Dashed lines are used to identify isomer bands.

Table 1. Reduced Mobility (K_o) and Collision Cross Section (CCS) Values in Nitrogen of ATHP $[M + 2H]^{2+}$, $[M + 3H]^{3+}$, and $[M + 4H]^{4+}$ Observed As a Function of the ESI Solvent Conditions

				decay ↓/growth ↑ lifetime (ms)	
isomer band	K_o ($cm^2\ V^{-1}s^{-1}$)	CCS [A^2]	ESI solution	ESI solvent condition II	ESI solvent condition III
$[M + 2H]^{2+}$ A	1.0878	370	III		↓ 650 ± 30
$[M + 2H]^{2+}$ B	1.0699	376	I, II, III	↓ 150 ± 40	↓ 650 ± 30
$[M + 2H]^{2+}$ C	1.0543	382	I, II, III	↑ 150 ± 50	↑ 650 ± 30
$[M + 2H]^{2+}$ D	1.0311	390	II	no variation	
$[M + 2H]^{2+}$ E	1.0241	393	I, III		no variation
$[M + 3H]^{3+}$ F	1.3891	435	I, II, III		↓ 100 ± 20
$[M + 3H]^{3+}$ G	1.3743	439	I, II, III		↓ 350 ± 30
$[M + 3H]^{3+}$ H	1.3487	448	I, II, III		↑ 350 ± 30
$[M + 3H]^{3+}$ I	1.3260	455	I, II, III		↑ 100 ± 20
$[M + 3H]^{3+}$ J	1.3051	463	III		↑ 100 ± 20
$[M + 4H]^{4+}$	1.4718	547	I, II, III		

adopt one conformation (e.g., m/z = 322, K_o = 1.376 $cm^2\ V^{-1}\ s^{-1}$, m/z = 622, K_o = 1.013 $cm^2\ V^{-1}\ s^{-1}$, and m/z = 922, K_o = 0.835 $cm^2\ V^{-1}\ s^{-1}$).[26]

Mobility, K, of an ion in the TIMS cell can be described by

$$K = \frac{v_g}{E} = \frac{A}{(V_{elution} - V_{base})} \quad (1)$$

where v_g, E, $V_{elution}$, and V_{base} are the velocity of the gas, applied electric field, elution and base voltages, respectively. The constant, A, is determined using standards of known mobilities under the same gas velocity conditions. The elution voltage, $V_{elution}$, can be calculated from the elution time:

$$V_{elution} = V_0 + r\frac{T_{elution}}{T_{ramp}} \quad (2)$$

and

$$T_{elution} = T_{total} - T_{trap} - TOF \quad (3)$$

where V_0 is the initial potential at the entrance to the TIMS analyzer, r is the rate at which the potential is ramped, $T_{elution}$ is the time at which the ion elutes, T_{ramp} is the total ramp time, T_{total} is the total time for a single TIMS experiment, T_{trap} is the time before the mobility analysis (i.e., to inject ions into the TIMS trap), and TOF is the time between elution of the ion and detection of the ion at the TOF detector. Mobility values (K) were correlated with CCS (Ω) using the equation:

$$\Omega = \frac{(18\pi)^{1/2}}{16}\frac{z}{(k_B T)^{1/2}}\left[\frac{1}{m_I} + \frac{1}{m_b}\right]^{1/2}\frac{1}{K}\frac{760}{P}\frac{T}{273.15}\frac{1}{N^*} \quad (4)$$

where z is the charge of the ion, k_B is the Boltzmann constant, N^* is the number density, and m_I and m_b refer to the masses of the molecular ion and bath gas molecule, respectively.

Molecular Dynamic Simulations. Conformational motifs were theoretically investigated using YASARA software (http://www.yasara.org). Briefly, simulations were performed using molecular mechanics (AMBER 03 force field) in a NVT thermostat that contains the molecular ion of interest interacting with nitrogen molecules. Typical simulation time was ~500 ps and multiple charge state and protonation sites (i.e., amine terminal, arginine and lysine) were considered. The

dx.doi.org/10.1021/ac403386q | Anal. Chem. 2014, 86, 1210−1214

influence of the charge location for the $[M + 2H]^{2+}$ and $[M + 3H]^{3+}$ is shown in the Supporting Information.

RESULTS AND DISCUSSION

Changes in the IMS profile, particularly the relative abundance of IMS bands, of ATHP were observed as a function of the ESI solvent conditions. Three ESI solution conditions are shown in Figure 1, water/methanol/acetonitrile (33:33:33), water/acetonitrile/acetic acid (49:49:2), and 10 mM ammonium acetate; from now on referred as ESI solvent conditions I, II, and III, respectively (see Table 1). Other solutions, including water/methanol (0:100−100:0) were also compared; however, similar results as ESI solvent condition II were obtained, thus results are not presented here. Inspection of Figure 1 shows that various ATHP conformational isomers are likely preserved during the ESI process and reflect the initial solvent state distribution as in previous studies utilizing bradykinin peptides.[23,28] Since CCS represents an "average" of the molecular ion surface that is accessible during collisions with the bath gas molecules, each IMS band corresponds to at least one conformational band (or family); that is, different conformations may yield the same CCS value. For example, ATHP $[M + 2H]^{2+}$ and $[M + 3H]^{3+}$ contain at least five conformation bands (labeled for each charge state), while ATHP $[M + 4H]^{4+}$ is dominated by a single broad band which is likely related to several conformations with very similar CCS values. When analyzed over time, changes in the IMS band distributions were observed for ATHP $[M + 2H]^{2+}$ and $[M + 3H]^{3+}$ but not for ATHP $[M + 4H]^{4+}$ regardless of the ESI solvent conditions. ESI solvent conditions I and II correspond to nonphysiological solvent states, and for simplicity, further comparisons were conducted between ESI solvent conditions II and III.

For the ATHP $[M + 2H]^{2+}$, the relative abundance of the IMS bands varied as a function of the trapping time and the ESI solvent conditions II and III (Figure 2). For ESI solvent condition II, the main pathway observed was B to C (150 ms conversion time). For ESI solvent condition III, the main pathway observed was A and B to C (650 ms growth time). Independent of ESI solvent condition, isomerization toward conformation C occurred, suggesting an overall higher stability for the "desolvated state" of ATHP $[M + 2H]^{2+}$ conformation C. For the ATHP $[M + 3H]^{3+}$, the relative abundance of the IMS bands varied as a function of the trapping time only for ESI solvent condition III; that is, no variations were observed for ESI conditions I and II (Figure 3). When analyzed as a function of the trapping time, two conformational interconversion pathways are observed: G to H (350 ms growth time) and F to J and I (100 ms growth time). We attribute the smaller variations for ATHP $[M + 3H]^{3+}$ to a lower flexibility of the conformational isomers at a higher charge state independent of the solution conditions. This behavior is consistent with the broad band observed for ATHP $[M + 4H]^{4+}$. That is, because of the small size of the molecule (decapeptide), intramolecular columbic repulsion (mainly between the Arg and Lys side chains) plays a larger role in the stabilization of the bulk molecular structure at higher charge states. In addition, heating of the conformational isomers was performed with the purpose of selectively annealing isomers into more stable forms by varying the ion effective temperature (i.e., rf amplitude 150−250 Vpp) during the trapping step in the TIMS cell. This approach is similar to collision activation experiments performed prior to IMS analysis[27,28] and may lead to the observation of gas-phase quasi-equilibrium distribution states by changing the ion effective temperature.[22,29−31] For ESI solvent conditions II and III, with the increase of the rf amplitude, the ATHP $[M + 2H]^{2+}$ and $[M + 3H]^{3+}$ charge state distributions shift to mainly C and H isomers, respectively. That is, the end step conformations obtained with the rf heating are the same as those that predominate in the trapping

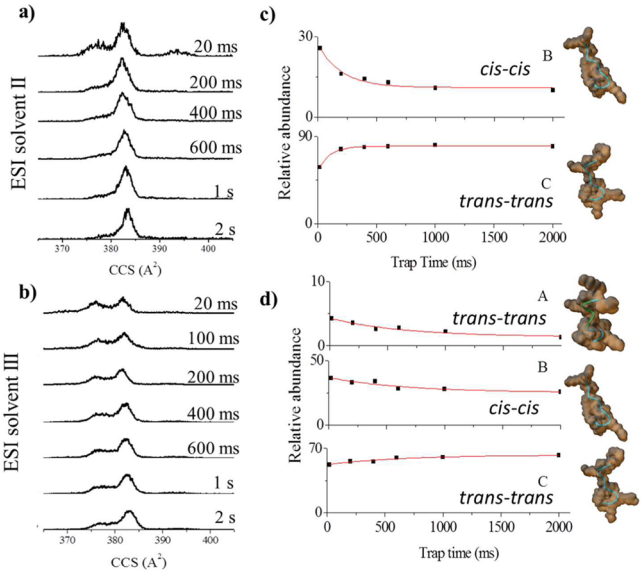

Figure 2. Typical ATHP $[M + 2H]^{2+}$ CCS profiles for ESI solvent conditions (a) II and (b) III as a function of the trap time (20 ms to 2 s). The relative abundances and candidate structures for the most abundant bands (A−C) as a function of the trap time is depicted in parts c and d for ESI solvent conditions II and III, respectively. Experimental data have been fitted with exponential decays. Candidate structures are displayed on the far right with the orientations of the proline residues presented.

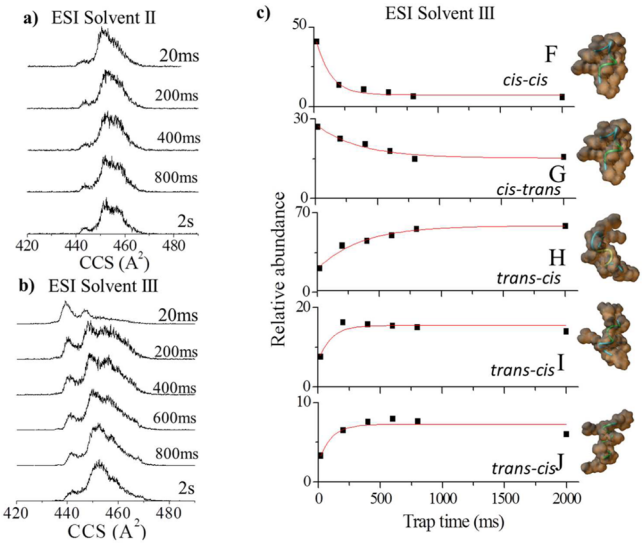

Figure 3. Typical ATHP $[M + 3H]^{3+}$ CCS profiles for ESI solvent conditions (a) II and (b) III as a function of the trap time (20 ms to 2 s). The relative abundances and candidate structures for the most abundant bands (F−J) as a function of the trap time is depicted in part c for ESI solvent condition III. Experimental data are fitted with exponential decays. Candidate structures are displayed on the far right with the orientations of the proline residues presented.

dx.doi.org/10.1021/ac403386q | Anal. Chem. 2014, 86, 1210−1214

experiments and more likely the more stable "desolvated" conformers.

Complementary information was obtained by theoretically studying the conformational dynamics of ATHP in the TIMS conditions (i.e., collisions with nitrogen molecules at a bath temperature of ~300 K). In particular, molecular dynamic simulations were used to investigate the interconversion dynamics as a function of the charge state and protonation site. From the simulations, candidate structures were proposed for the isomer bands observed for the ATHP $[M + 2H]^{+}$ and the $[M + 3H]^{+}$ distributions (Figures 2 and 3, respectively). The ATHP $[M + 2H]^{2+}$ conformational interconversion follows different mechanisms. That is, it can be a result of relaxation in the peptide backbone (interconversion of band A to D), reorientation of side chains (interconversion of band E to D), and a combination of these two mechanisms (interconversion of band B to C). For ATHP $[M + 3H]^{3+}$, the main differences between the candidate structures also arises from changes in the backbone, side-chain orientation, and protonation site. Previous solution phase NMR experiments showed that ATHP binding does not significantly perturb the DNA conformation in the "AT-hook motif" and that all proline residues are in the trans conformation (similar to conformation C).[11,32] The central RGR core deeply penetrates to the minor groove of AT base pairs and forms extensive electrostatic and hydrophobic contacts with the floor of the minor groove. The two prolines direct the motif away from the floor of the minor groove and place the positively charged amino acids near the negatively charged phosphate backbone making further contacts with DNA.[11] However, a small population of peptides with *cis*-proline isomers was also observed in good agreement with the candidate structures proposed in Figures 2 and 3.[32] The relative stability of the conformational isomers proposed in Figures 2 and 3 are also in good agreement with the NMR observations. That is, the all trans-proline conformation is the more stable, and stability decreases with the increase of cis-proline isomers. Similar backbone stabilization of the conformational space in proline containing peptides has been previously observed.[22,23,28]

CONCLUSIONS

In solution, ATHP conformations are expected to be selectively stabilized by the solvent conditions and by specific binding to the DNA portion. Previous observation of multiple structures[16,32] and the results presented here provide a means to better describe the interaction dynamics of ATHP folding and ATHP desolvation. The results presented here also showed that TIMS-MS is a valuable tool to investigate solvent states and that isomerization kinetics can be followed at the level of side chain interaction and backbone relaxation. It is also shown that ATHP is "structured" and that ATHP conformations are defined by the protonation site, backbone, and side orientations and can retain the memory of the initial solvent distribution during desolvation.

ASSOCIATED CONTENT

Supporting Information

PDB files of the ATHP candidate structures proposed and a table containing the proline residue isomerization, protonation site, and relative energy. This material is available free of charge via the Internet at http://pubs.acs.org.

AUTHOR INFORMATION

Corresponding Author

*Phone: 305-348-2037. Fax: 305-348-3772. E-mail: fernandf@fiu.edu.

Notes

The authors declare no competing financial interest.

ACKNOWLEDGMENTS

This work was supported by National Institute of Health (Grant No. R00GM106414 to F.F.-L. and Grant No. 5SC1HD063059-04 To F.L.). The authors wish to acknowledge Dr. Desmond Kaplan from Bruker Daltonics Inc. for the development of TIMS acquisition software.

REFERENCES

(1) Young, A. R.; Narita, M. *Genes Dev.* **2007**, *21*, 1005−1009.
(2) Morishita, A.; Zaidi, M. R.; Mitoro, A.; Sankarasharma, D.; Szabolcs, M.; Okada, Y.; D'Armiento, J.; Chada, K. *Cancer Res.* **2013**, *73*, 4289−4299.
(3) Zhou, X.; Benson, K. F.; Ashar, H. R.; Chada, K. *Nature* **1995**, *376*, 771−774.
(4) Anand, A.; Chada, K. *Nat. Genet.* **2000**, *24*, 377−380.
(5) Weedon, M. N.; Lettre, G.; Freathy, R. M.; Lindgren, C. M.; Voight, B. F.; Perry, J. R.; Elliott, K. S.; Hackett, R.; Guiducci, C.; Shields, B.; Zeggini, E.; Lango, H.; Lyssenko, V.; Timpson, N. J.; Burtt, N. P.; Rayner, N. W.; Saxena, R.; Ardlie, K.; Tobias, J. H.; Ness, A. R.; Ring, S. M.; Palmer, C. N.; Morris, A. D.; Peltonen, L.; Salomaa, V.; Davey Smith, G.; Groop, L. C.; Hattersley, A. T.; McCarthy, M. I.; Hirschhorn, J. N.; Frayling, T. M. *Nat. Genet.* **2007**, *39*, 1245−1250.
(6) Horikoshi, M.; Yaghootkar, H.; Mook-Kanamori, D. O.; Sovio, U.; Taal, H. R.; Hennig, B. J.; Bradfield, J. P.; St. Pourcain, B.; Evans, D. M.; Charoen, P.; Kaakinen, M.; Cousminer, D. L.; Lehtimaki, T.; Kreiner-Moller, E.; Warrington, N. M.; Bustamante, M.; Feenstra, B.; Berry, D. J.; Thiering, E.; Pfab, T.; Barton, S. J.; Shields, B. M.; Kerkhof, M.; van Leeuwen, E. M.; Fulford, A. J.; Kutalik, Z.; Zhao, J. H.; den Hoed, M.; Mahajan, A.; Lindi, V.; Goh, L. K.; Hottenga, J. J.; Wu, Y.; Raitakari, O. T.; Harder, M. N.; Meirhaeghe, A.; Ntalla, I.; Salem, R. M.; Jameson, K. A.; Zhou, K.; Monies, D. M.; Lagou, V.; Kirin, M.; Heikkinen, J.; Adair, L. S.; Alkuraya, F. S.; Al-Odaib, A.; Amouyel, P.; Andersson, E. A.; Bennett, A. J.; Blakemore, A. I.; Buxton, J. L.; Dallongeville, J.; Das, S.; de Geus, E. J.; Estivill, X.; Flexeder, C.; Froguel, P.; Geller, F.; Godfrey, K. M.; Gottrand, F.; Groves, C. J.; Hansen, T.; Hirschhorn, J. N.; Hofman, A.; Hollegaard, M. V.; Hougaard, D. M.; Hypponen, E.; Inskip, H. M.; Isaacs, A.; Jorgensen, T.; Kanaka-Gantenbein, C.; Kemp, J. P.; Kiess, W.; Kilpelainen, T. O.; Klopp, N.; Knight, B. A.; Kuzawa, C. W.; McMahon, G.; Newnham, J. P.; Niinikoski, H.; Oostra, B. A.; Pedersen, L.; Postma, D. S.; Ring, S. M.; Rivadeneira, F.; Robertson, N. R.; Sebert, S.; Simell, O.; Slowinski, T.; Tiesler, C. M.; Tonjes, A.; Vaag, A.; Viikari, J. S.; Vink, J. M.; Vissing, N. H.; Wareham, N. J.; Willemsen, G.; Witte, D. R.; Zhang, H.; Zhao, J.; Wilson, J. F.; Stumvoll, M.; Prentice, A. M.; Meyer, B. F.; Pearson, E. R.; Boreham, C. A.; Cooper, C.; Gillman, M. W.; Dedoussis, G. V.; Moreno, L. A.; Pedersen, O.; Saarinen, M.; Mohlke, K. L.; Boomsma, D. I.; Saw, S. M.; Lakka, T. A.; Korner, A.; Loos, R. J.; Ong, K. K.; Vollenweider, P.; van Duijn, C. M.; Koppelman, G. H.; Hattersley, A. T.; Holloway, J. W.; Hocher, B.; Heinrich, J.; Power, C.; Melbye, M.; Guxens, M.; Pennell, C. E.; Bonnelykke, K.; Bisgaard, H.; Eriksson, J. G.; Widen, E.; Hakonarson, H.; Uitterlinden, A. G.; Pouta, A.; Lawlor, D. A.; Smith, G. D.; Frayling, T. M.; McCarthy, M. I.; Grant, S. F.; Jaddoe, V. W.; Jarvelin, M. R.; Timpson, N. J.; Prokopenko, I.; Freathy, R. M. *Nat. Genet.* **2013**, *45*, 76−82.
(7) Copley, M. R.; Babovic, S.; Benz, C.; Knapp, D. J.; Beer, P. A.; Kent, D. G.; Wohrer, S.; Treloar, D. Q.; Day, C.; Rowe, K.; Mader, H.; Kuchenbauer, F.; Humphries, R. K.; Eaves, C. J. *Nat. Cell Biol.* **2013**, *15*, 916−25.

(8) Stein, J. L.; Medland, S. E.; Vasquez, A. A.; Hibar, D. P.; Senstad, R. E.; Winkler, A. M.; Toro, R.; Appel, K.; Bartecek, R.; Bergmann, O.; Bernard, M.; Brown, A. A.; Cannon, D. M.; Chakravarty, M. M.; Christoforou, A.; Domin, M.; Grimm, O.; Hollinshead, M.; Holmes, A. J.; Homuth, G.; Hottenga, J. J.; Langan, C.; Lopez, L. M.; Hansell, N. K.; Hwang, K. S.; Kim, S.; Laje, G.; Lee, P. H.; Liu, X.; Loth, E.; Lourdusamy, A.; Mattingsdal, M.; Mohnke, S.; Maniega, S. M.; Nho, K.; Nugent, A. C.; O'Brien, C.; Papmeyer, M.; Putz, B.; Ramasamy, A.; Rasmussen, J.; Rijpkema, M.; Risacher, S. L.; Roddey, J. C.; Rose, E. J.; Ryten, M.; Shen, L.; Sprooten, E.; Strengman, E.; Teumer, A.; Trabzuni, D.; Turner, J.; van Eijk, K.; van Erp, T. G.; van Tol, M. J.; Wittfeld, K.; Wolf, C.; Woudstra, S.; Aleman, A.; Alhusaini, S.; Almasy, L.; Binder, E. B.; Brohawn, D. G.; Cantor, R. M.; Carless, M. A.; Corvin, A.; Czisch, M.; Curran, J. E.; Davies, G.; de Almeida, M. A.; Delanty, N.; Depondt, C.; Duggirala, R.; Dyer, T. D.; Erk, S.; Fagerness, J.; Fox, P. T.; Freimer, N. B.; Gill, M.; Goring, H. H.; Hagler, D. J.; Hoehn, D.; Holsboer, F.; Hoogman, M.; Hosten, N.; Jahanshad, N.; Johnson, M. P.; Kasperaviciute, D.; Kent, J. W., Jr.; Kochunov, P.; Lancaster, J. L.; Lawrie, S. M.; Liewald, D. C.; Mandl, R.; Matarin, M.; Mattheisen, M.; Meisenzahl, E.; Melle, I.; Moses, E. K.; Muhleisen, T. W.; Nauck, M.; Nothen, M. M.; Olvera, R. L.; Pandolfo, M.; Pike, G. B.; Puls, R.; Reinvang, I.; Renteria, M. E.; Rietschel, M.; Roffman, J. L.; Royle, N. A.; Rujescu, D.; Savitz, J.; Schnack, H. G.; Schnell, K.; Seiferth, N.; Smith, C.; Steen, V. M.; Valdes Hernandez, M. C.; Van den Heuvel, M.; van der Wee, N. J.; Van Haren, N. E.; Veltman, J. A.; Volzke, H.; Walker, R.; Westlye, L. T.; Whelan, C. D.; Agartz, I.; Boomsma, D. I.; Cavalleri, G. L.; Dale, A. M.; Djurovic, S.; Drevets, W. C.; Hagoort, P.; Hall, J.; Heinz, A.; Jack, C. R., Jr.; Foroud, T. M.; Le Hellard, S.; Macciardi, F.; Montgomery, G. W.; Poline, J. B.; Porteous, D. J.; Sisodiya, S. M.; Starr, J. M.; Sussmann, J.; Toga, A. W.; Veltman, D. J.; Walter, H.; Weiner, M. W.; Bis, J. C.; Ikram, M. A.; Smith, A. V.; Gudnason, V.; Tzourio, C.; Vernooij, M. W.; Launer, L. J.; DeCarli, C.; Seshadri, S.; Andreassen, O. A.; Apostolova, L. G.; Bastin, M. E.; Blangero, J.; Brunner, H. G.; Buckner, R. L.; Cichon, S.; Coppola, G.; de Zubicaray, G. I.; Deary, I. J.; Donohoe, G.; de Geus, E. J.; Espeseth, T.; Fernandez, G.; Glahn, D. C.; Grabe, H. J.; Hardy, J.; Hulshoff Pol, H. E.; Jenkinson, M.; Kahn, R. S.; McDonald, C.; McIntosh, A. M.; McMahon, F. J.; McMahon, K. L.; Meyer-Lindenberg, A.; Morris, D. W.; Muller-Myhsok, B.; Nichols, T. E.; Ophoff, R. A.; Paus, T.; Pausova, Z.; Penninx, B. W.; Potkin, S. G.; Samann, P. G.; Saykin, A. J.; Schumann, G.; Smoller, J. W.; Wardlaw, J. M.; Weale, M. E.; Martin, N. G.; Franke, B.; Wright, M. J.; Thompson, P. M. *Nat. Genet.* **2012**, *44*, 552−61.
(9) Cui, T.; Leng, F. *Biochemistry* **2007**, *46*, 13059−13066.
(10) Lehn, D. A.; Elton, T. S.; Johnson, K. R.; Reeves, R. *Biochem. Int.* **1988**, *16*, 963−971.
(11) Huth, J. R.; Bewley, C. A.; Nissen, M. S.; Evans, J. N.; Reeves, R.; Gronenborn, A. M.; Clore, G. M. *Nat. Struct. Biol.* **1997**, *4*, 657−65.
(12) Reeves, R. *Biochem. Cell Biol.* **2003**, *81*, 185−195.
(13) Reeves, R. *Gene* **2001**, *277*, 63−81.
(14) Fenn, J.; Mann, M.; Meng, C.; Wong, S.; Whitehouse, C. *Science* **1989**, *246*, 64−71.
(15) Kanu, A. B.; Dwivedi, P.; Tam, M.; Matz, L.; Hill, H. H. *J. Mass Spectrom.* **2008**, *43*, 1−22.
(16) Tao, L.; McLean, J. R.; McLean, J. A.; Russell, D. H. *J. Am. Soc. Mass Spectrom.* **2007**, *18*, 1232−1238.
(17) Valentine, S. J.; Counterman, A. E.; Clemmer, D. E. *J. Am. Soc. Mass Spectrom.* **1999**, *10*, 1188−1211.
(18) Ruotolo, B. T.; Benesch, J. L. P.; Sandercock, A. M.; Hyung, S.-J.; Robinson, C. V. *Nat. Protoc.* **2008**, *3*, 1139−1152.
(19) Fernandez-Lima, F. A.; Blase, R. C.; Russell, D. H. *Int. J. Mass Spectrom.* **2010**, *298*, 111−118.
(20) Beveridge, R.; Chappuis, Q.; Macphee, C.; Barran, P. *Analyst* **2013**, *138*, 32−42.
(21) Wyttenbach, T.; von Helden, G.; Bowers, M. T. *J. Am. Chem. Soc.* **1996**, *118*, 8355−8364.
(22) Fernandez-Lima, F. A.; Wei, H.; Gao, Y. Q.; Russell, D. H. *J. Phys. Chem. A* **2009**, *113*, 8221−8234.
(23) Pierson, N. A.; Chen, L.; Valentine, S. J.; Russell, D. H.; Clemmer, D. E. *J. Am. Chem. Soc.* **2011**, *133*, 13810−13813.
(24) Fernandez-Lima, F. A.; Kaplan, D. A.; Suetering, J.; Park, M. A. *Int. J. Ion Mobil. Spectrom.* **2011**, *14*, 93−98.
(25) Fernandez-Lima, F. A.; Kaplan, D. A.; Park, M. A. *Rev. Sci. Instrum.* **2011**, *82*, 126106.
(26) United States, 1999.
(27) Pierson, N. A.; Valentine, S. J.; Clemmer, D. E. *J. Phys. Chem. B* **2010**, *114*, 7777−7783.
(28) Pierson, N. A.; Chen, L.; Russell, D. H.; Clemmer, D. E. *J. Am. Chem. Soc.* **2013**, *135*, 3186−3192.
(29) Wysocki, V. H.; Kenttämaa, H. I.; Cooks, R. G. *Int. J Mass Spectrom. Ion Processes* **1987**, *75*, 181−208.
(30) Donald, W. A.; Khairallah, G. N.; O'Hair, R. A. *J Am. Soc. Mass Spectrom.* **2013**, *24*, 811−815.
(31) Robinson, E. W.; Shvartsburg, A. A.; Tang, K.; Smith, R. D. *Anal. Chem.* **2008**, *80*, 7508−7515.
(32) Geierstanger, B. H.; Volkman, B. F.; Kremer, W.; Wemmer, D. E. *Biochemistry* **1994**, *33*, 5347−5355.